Boron-Catalyzed Electrochemical Si–C Bond Formation for Safe and Controllable Benzylation and Allylation of Hydrosilanes

Alexander D. Beck,[a, b] Stefan Haufe,[a] and Siegfried R. Waldvogel*[b]

The range of possible applications of $B(C_6F_5)_3$ extends into many areas of organic and inorganic chemistry. However, electrochemical synthesis with hydrosilanes using $B(C_6F_5)_3$ to increase yield or scope has not yet been achieved. A comprehensive study on the use of Lewis acidic boron species, especially $B(C_6F_5)_3$, for the activation of hydrosilanes in presence of commercially available supporting electrolyte for Si–C bond formation was presented. The benzylation and allylation of hydrosilane species was successfully conducted in presence of catalytic amounts of $B(C_6F_5)_3$ in yields up to 86%. Screening of electrode materials revealed leaded bronzes as superior for cathodic conversion without contamination of the electrolyte by heavy metals. Supported by cyclic voltammetry studies, $B(C_6F_5)_3$ activated the hydrosilane for easier nucleophilic access, leading to significant increase in yield and enrichment of the target product in the reaction mixture.

Introduction

Tris(pentafluorophenyl)borane, $B(C_6F_5)_3$, has been subject to numerous applications in organic[1,2] and inorganic chemistry[3] since its discovery in 1963.[4] It is a powerful Lewis acid comparable to BF_3 or BCl_3,[5] but unlike these boron halides, it is an easy-to-handle, and a quite thermally stable solid. Due to its high steric demand, $B(C_6F_5)_3$ is incapable to form dative bonds in acid-base adducts despite its high Lewis acidity.[6] This feature has been associated with the term "frustrated Lewis pair" (FLP) chemistry,[6] which opens up new reaction pathways and possibilities, as demonstrated by the activation of small molecules like H_2,[6,7,8,9] CO,[6,7,9,10] CO_2[6,7,9,11] etc.

In addition, the activation of Si–H bonds with $B(C_6F_5)_3$ is possible. In contrast to common Lewis acid activation of carbonyl moieties, $B(C_6F_5)_3$ does not coordinate the carbonyl oxygen, which polarizes the double bond and generates a highly electrophilic carbon. The electron withdrawing $B(C_6F_5)_3$ **I** rather forms an adduct **II** with the hydrosilane,[12] and may partially abstract the hydride (Scheme 1).[13–15] By nucleophilic attack of a carbonyl oxygen at the silicon center, the activated hydrosilane forms a borohydride stabilized ion pair **III**, that releases $B(C_6F_5)_3$ to close the catalytic cycle by hydride transfer to accomplish the silyl ether species.

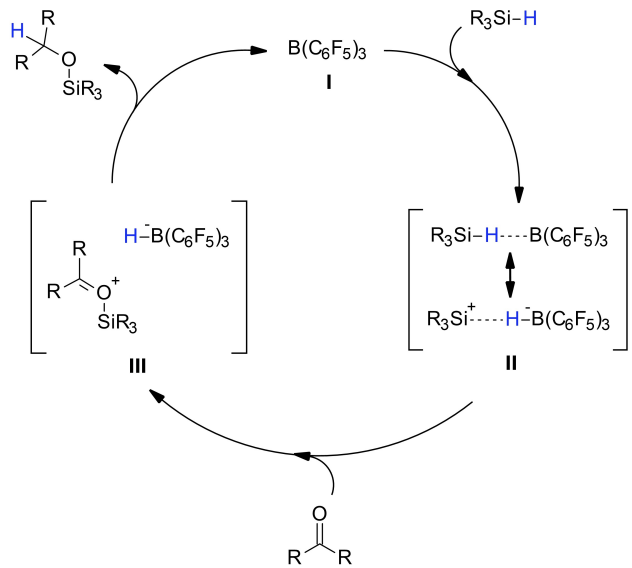

Scheme 1. Activation of hydrosilane by $B(C_6F_5)_3$ and subsequent hydrosilylation of carbonyl compounds with regeneration of $B(C_6F_5)_3$.[12,13,15–17]

This key discovery of a metal-free hydrosilane activation by $B(C_6F_5)_3$ has been of significant interest within the past 20 years. The range of application for $B(C_6F_5)_3$ has greatly expanded and several catalytic silane-based transformations e.g. silylation of alcohols,[18] hydrosilylation of aldehydes,[19] alkenes,[20,21] alkynes,[21] enols,[22] esters,[19] imines,[14,17,23] and ketones,[17,19,24] the chlorination of hydrosilanes to respective chlorosilanes[25] and deoxygenation of alcohols[1,26] and carbonyl compounds.[26] have been reported so far.

Recently, this unique boron compound has expanded into the field of electrochemistry. Studies on the reduction potential of $B(C_6F_5)_3$,[27,28] as well as electrosynthetic aspects, especially

[a] A. D. Beck, Dr. S. Haufe
Consortium für elektrochemische Industrie
Wacker Chemie AG
Zielstattstraße 20, 81379 München (Germany)
[b] A. D. Beck, Prof. Dr. S. R. Waldvogel
Department Chemie
Johannes Gutenberg-Universität Mainz
Duesbergweg 10–14, 55128 Mainz (Germany)
E-mail: waldvogel@uni-mainz.de
Homepage: https://www.aksw.uni-mainz.de/

Supporting information for this article is available on the WWW under https://doi.org/10.1002/celc.202200840

© 2022 The Authors. ChemElectroChem published by Wiley-VCH GmbH. This is an open access article under the terms of the Creative Commons Attribution Non-Commercial NoDerivs License, which permits use and distribution in any medium, provided the original work is properly cited, the use is non-commercial and no modifications or adaptations are made.

© 2022 The Authors. ChemElectroChem published by Wiley-VCH GmbH

21960216, 2022, 17, Downloaded from https://chemistry-europe.onlinelibrary.wiley.com/doi/10.1002/celc.202200840 by Universitatsbibliothek Mainz, Wiley Online Library on [27/01/2023]. See the Terms and Conditions (https://onlinelibrary.wiley.com/terms-and-conditions) on Wiley Online Library for rules of use; OA articles are governed by the applicable Creative Commons License

with respect to the activation of hydrogen,[29,30] have been the focus of such research. Previous studies indicate that $B(C_6F_5)_3$ is deactivated in electrolytes containing coordinating anions such as perchlorate.[28,31] This phenomenon is exploited by the use of $B(C_6F_5)_3$ as anion receptor in lithium-ion batteries to stabilize the solid-electrolyte-interphase (SEI),[32] and to inhibit the electrolyte decomposition by anion complexation.[33]

Notwithstanding, we have recently shown that anion receptor function of $B(C_6F_5)_3$ does not appear to be an irreversible, deactivating type of complexation in the presence of perchlorate.[34] This has led to the case of a $B(C_6F_5)_3$ mediated silicon based organic electrochemistry. As our results revealed, a catalytic activity of $B(C_6F_5)_3$ is detectable in presence of perchlorate anion, indicating a mediator role. In this case, the amount of applied charge required for intended oxidative Si–Si bond formation decreases by more than half in the presence of 2.5 mol% $B(C_6F_5)_3$. This suggests an alternative reaction pathway. However, to the best of our knowledge, $B(C_6F_5)_3$ has not yet been applied to increase yield or scope for the electrochemical Si bond formation. Here, we present the first study to successfully apply $B(C_6F_5)_3$ as mediator in electrochemical silane-based synthesis regarding Si–C bond formation, increasing yield and substrate scope for an exemplary benzylation and allylation of hydrosilane species.

Allylation of silanes has been an interest of (electro) organic synthesis for many years, due to easy subsequent functionalization,[35] and synthetic application in production of pharmaceutically active compounds.[36] Over this period, various approaches to the corresponding allylsilanes have been established: Grignard related Sm-mediated systems,[37] the Pd-catalyzed cleavage of disilanes and reaction with trifluoroacetate,[38] as well as the electrochemical reduction of the corresponding organic halides in presence of chlorosilanes (Scheme 2, top).[39–41]

The benzylation of silanes by Grignard reagents reacting with chlorosilanes to form the respective Si–C bond is known for over 100 years.[42] It has further gained attraction in the electrochemical,[39] as well as in the Pd-catalyzed field of organic chemistry (Scheme 2, bottom).[43] Benzylsilanes are used as organosilicon fragments in organic synthesis.[44] While conventional synthetic protocols need stoichiometric or even larger amounts of oxidizers or reducing agents, electrochemistry provides a green alternative.[45] In particular, reagent waste is avoided and if renewable electricity is applied such processes become very sustainable.[46] In addition, the reaction occurs close to the electrode and the simple switch-off for the electric power prevent thermal runaway reactions and makes this technology inherently safe.[47]

However, the reduction of chlorosilanes and organic halides in aprotic media leads to electrolyte halogenation in the absence of a halide scavenger, which does not allow the reaction to be defined as sustainable. Due to this circumstance, we may report an electrochemical reaction pathway with $B(C_6F_5)_3$ mediator, allowing the oxidation of hydrosilanes to the corresponding allyl- or benzylsilanes and suppressing solvent chlorination.

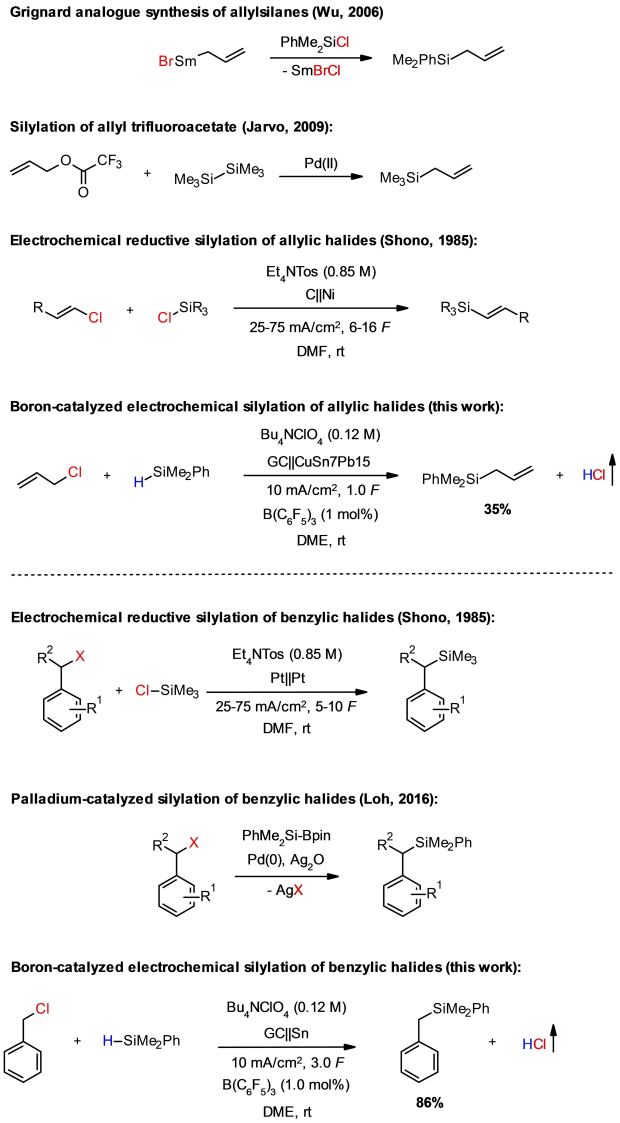

Scheme 2. Strategies for the synthesis of allylsilanes;[37–41] (top) and benzylsilanes,[39,43] (bottom) Tos = *p*-toluenesulfonate, DMF = *N*,*N*-dimethylformamide, GC = glassy carbon, DME = 1,2-dimethoxyethane, Bpin = 4,4,5,5-tetramethyl-1,3,2-dioxaborolane.

Results and Discussion

Electrochemical reduction of halosilanes and organic halides involves cleavage of free halides, which must be removed from the reaction process to prevent halogenation of the aprotic solvent. In the past, this was often achieved by the use of sacrificial metal anodes, such as magnesium,[48] copper[49] or mercury,[50] which form the corresponding insoluble metal halides. Alternatively, non-sacrificial anode materials have been tested.[51] The use of proton releasing species for halogen scavenging to generate hydrogen chloride, which can be removed during the reaction, is scarce in silicon based electrochemistry. One option for oxidative proton generation is anodic conversion of hydrosilanes. This represents an environmentally friendlier alternative without the formation of metal chlorides. Inspired by this oxidative electrochemical transformation of

© 2022 The Authors. ChemElectroChem published by Wiley-VCH GmbH

21960216, 2022, 17, Downloaded from https://chemistry-europe.onlinelibrary.wiley.com/doi/10.1002/celc.202200840 by Universitatsbibliothek Mainz, Wiley Online Library on [27/01/2023]. See the Terms and Conditions (https://onlinelibrary.wiley.com/terms-and-conditions) on Wiley Online Library for rules of use; OA articles are governed by the applicable Creative Commons License

21960216, 2022, 17, Downloaded from https://chemistry-europe.onlinelibrary.wiley.com/doi/10.1002/celc.202200840 by Universitatsbibliothek Mainz, Wiley Online Library on [27/01/2023]. See the Terms and Conditions (https://onlinelibrary.wiley.com/terms-and-conditions) on Wiley Online Library for rules of use; OA articles are governed by the applicable Creative Commons License

hydrosilanes, as reported by Kunai *et al.* for the Si–Si bond formation in presence of chlorosilanes to form the respective disilanes (Scheme 3, top),[52] we utilized this combined electrochemical transformation to generate Si–C bonds under the release of hydrogen chloride. In analogy we used the hydrosilane dimethylphenylsilane (Me_2PhSi–H, **1**) for an oxidative cleavage of the Si–H bond to form the respective silyl cation. At the same time, reduction of an organic halide allows for the Si–C bond formation (Scheme 3, bottom).

Screening of solvent, electrode materials and stoichiometry of starting materials revealed, that the reaction suffers from a lack of selectivity and thus forms chlorodimethylphenylsilane (Me_2PhSi–Cl, **2**) and tetramethyldiphenyldisiloxane (Me_2PhSi–O–$SiMe_2Ph$, **3**) as by-products (see Supporting Information). The depicted reaction conditions show a maximum yield of 10% for the benzylation of hydrosilane to benzyldimethylphenylsilane (Me_2PhSi–Bn, **4**). Conversion of starting material is low, especially in the case of benzyl chloride. In addition to the desired benzylsilane **4**, C–H bond formation and chlorination of the solvent occur, indicating an anodic competition of chloride ions to the oxidation of hydrosilane,

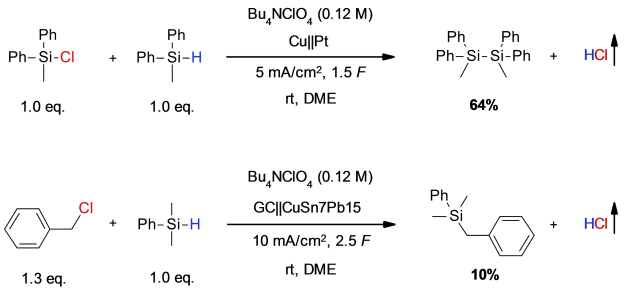

Scheme 3. Direct Si–Si bond formation via oxidation of hydrosilane (top),[52] analogue oxidative coupling for Si–C bond formation of this work (bottom), DME = 1,2-dimethoxyethane, GC = glassy carbon.

Table 1. Product yield for the catalyzed and non-catalyzed oxidative Si–C bond formation.

Entry	Lewis acid	Mol%	Si–C, **4** Yield[b]	Si–Cl, **2** Yield[b]	Si–O, **3** Yield[b]	Conversion[a]
1[c]	None	0.0	10%	6%	2%	22%
2[c]	$B(C_6F_5)_3$	1.0	51%	39%	6%	100%
3[c]	$B(C_6F_5)_3$	2.5	49%	36%	14%	100%
4[c]	$B(C_6F_5)_3$	5.0	46%	34%	20%	100%
5[d]	$B(C_6F_5)_3$	1.0	0%	0%	1%	1%
6[d]	$B(C_6F_5)_3$	2.5	0%	0%	4%	4%
7[d]	$B(C_6F_5)_3$	5.0	0%	0%	7%	7%
8[e]	$B(C_6F_5)_3$	1.0	67%	21%	8%	100%
9[e]	BCl_3	1.0	25%	25%	4%	56%
10[e]	BEt_3	1.0	58%	36%	3%	100%
11[e]	$AlCl_3$	1.0	2%	6%	5%	13%
12[e]	None	0.0	12%	7%	3%	23%

[a] Reaction conditions: 1,2-dimethoxyethane as solvent with 0.12 M Bu_4NClO_4 supporting electrolyte, anode material is glassy carbon, cathode material is CuSn7Pb15, Me_2PhSiH (0.50 M, 2.5 mmol) and benzyl chloride (0.69 M, 3.43 mmol), at room temperature. [b] Yield determined by NMR referenced to TMS; Si–C, 4 = benzyldimethylphenylsilane; Si–Cl, 2 = chlorodimethylphenylsilane; Si–O, 3 = tetramethyldiphenyldisiloxane. [c] Current density of 10 mA/cm^2, applied charge of 1.0 *F*. [d] Without electric current. [e] Current density of 10 mA/cm^2, applied charge of 3.0 *F*.

due to a peak potential of hydrosilane **1** of 2.07 V vs. FcH/FcH^+ (Ferrocene / Ferrocenium) (*vide infra*). Comparable results are obtained by using alkyl halides, such as 1-chlorooctane, and aryl halides, like chlorobenzene. The yield of Si–C bond formation increases with increasing stabilization of the corresponding carbanion intermediate, showing benzylsilane **4** as the product of highest yield with 10% to be obtained so far (Table 1, entry 1).

As we have recently shown,[34] $B(C_6F_5)_3$ represents a possibility for Si–H bond activation even in the presence of perchlorate. Based on these studies, we have investigated the use of $B(C_6F_5)_3$ for oxidative Si–C bond formation. By addition of a catalytic amount of 1.0 mol% $B(C_6F_5)_3$ to the reaction mixture, 100% conversion and an increase in yield of benzylsilane **4** to 51% is achieved (Table 1, entry 2). With increasing amount of $B(C_6F_5)_3$, the product distribution is shifted to disiloxane **3** (Table 1, entries 2–4), probably due to the high reactivity of the activated hydrosilane in presence of the perchlorate species. Nucleophilic access and decomposition of perchlorate leads to subsequent formation of disiloxane **3**. In a current-less state, no Si–C bond formation is obtained and regardless of reaction time, only a minor amount of hydrosilane **1** is converted to form disiloxane **3**, the yield of which increases with the amount of $B(C_6F_5)_3$ used (Table 1, entries 5–7).

We extended the hydrosilane activation for electrochemical Si–C bond formation to additional borane species and Lewis acids. Besides $B(C_6F_5)_3$, BCl_3 and BEt_3 allow for a successful catalytic activation of Si–H bonds in presence of perchlorate although $B(C_6F_5)_3$ provides the highest yield of benzylsilane **4** for an applied charge of 3.0 *F* (Table 1, entry 8). Conversion and yield for BCl_3 are significantly diminished (Table 1, entry 9), due to complexation of chloride ions by the high Lewis acidic and relatively minor steric demanding BCl_3. Still, an increase in yield of more than two-fold compared to the non-catalyzed reaction pathway shows its potential for Si–H bond activation in presence of perchlorate. BEt_3 generates almost comparable results to $B(C_6F_5)_3$, yielding 58% of benzylsilane **4** with full conversion of the hydrosilane species (Table 1, entry 10). BEt_3 is known as a radical initiator for the hydrosilylation of electron-rich alkenes,[53] indicating an aspect for a possible one-electron process of the activated Si–C bond formation. Leaving the field of borane chemistry and entering aluminum related Lewis acids, $AlCl_3$ does not only show missing ability for Si–H bond activation (Table 1, entry 11). Moreover, the yield and conversion decrease compared to the product distribution of the non-activated route. A redox shuttle functionality of $AlCl_3$ is supposed, with charge amount being consumed by alternating oxidation and reduction of the aluminum species without conversion of the desired silyl species. In absence of the Lewis acid, reduction of benzyl chloride with subsequent oxidation of released chloride occurs. Due to the high oxidation potential of hydrosilane **1**, solvent chlorination is the main reaction, leading to low hydrosilane conversion (Table 1, entry 12).

The presence of a coordinating anion such as perchlorate is mandatory to stabilize the reactive, activated silyl species, otherwise a quantitative catalytic reaction of hydrosilane **1** with the solvent 1,2-dimethoxyethane occurs at room temperature.

© 2022 The Authors. ChemElectroChem published by Wiley-VCH GmbH

The solvent is converted to the corresponding silyl ether (2-methoxyethoxy)dimethylphenylsilane ($Me_2PhSi–OCH_2CH_2OMe$, **5**) in 96% yield under elimination of methane (Scheme 4, path **I**). Various perchlorate and tetrafluoroborate supporting electrolytes prevent this catalytic process with only minor conversion of hydrosilane **1** to the corresponding disiloxane **3** for perchlorate or fluorosilane in case of tetrafluoroborate supporting electrolyte (see Supporting Information). Is the boron activated hydrosilane in a stabilized state due to the coordinating anion (Scheme 4, path **II**), access for nucleophilic attack at the silicon center is facilitated. A carbanion generated via cathodic reduction can easily form the respective Si–C bond. A competing reaction of the released chloride ion leads to the formation of a chlorosilane compound. By consecutive oxidation, the Lewis acidic boron species is regenerated to be ready for further hydrosilane activation under the release of protons. The mediator, in addition to the role of activating the hydrosilane species for nucleophilic attack, further fulfills the function of oxidative protection of the supporting electrolyte. As indicated by cyclic voltammetry measurements (*vide infra*) the oxidation potential of the intermediate is shifted to the less anodic values, thus preventing oxidation of chloride and subsequent solvent halogenation. Anodic hydrogen evolution could not be detected in course of reaction, indicating the formation of hydrogen chloride, dissolved in the supporting electrolyte.

To gain deeper insight into the reaction process and conversion, we analyzed the reaction mixture with increasing applied charge by GC and NMR. An interesting picture emerges, which can be divided into two sections (Figure 1): In the first section, up to 1.0 *F*, the reaction is driven by the activated hydrosilane **1**. Conversion leads to benzylsilane **4** as main product and the corresponding chlorosilane **2** as by-product. A small initial amount of disiloxane **3** is formed, probably due to decomposition of the activated silyl species with the supporting electrolyte, that does not further increase as the reaction proceeds. Formation of disiloxane **3** is not electrochemical induced for the benzylation of hydrosilanes.

At 1.0 *F* hydrosilane **1** is completely consumed, marking the transition to the second process section: Benzylsilane **4** continues to be formed, since the benzyl chloride concentration is at about 50% of its initial amount and available for further reduction. In this case, however, the organic halide reacts with chlorosilane **2** instead of hydrosilane **1**, diminishing the amount of chlorosilane in the course of reaction and increasing the yield of benzylsilane **4** up to 67%. Beyond 3.0 *F*, solvent chlorination occurs, and the reaction is discontinued.

Analysis of the product distribution with increasing applied charge leads to two observations: the investigated borane-activated electrochemical conversion indicates a single-electron process, allowing for the complete conversion of hydrosilane **1** after 1.0 *F*. Second, these results show a possible formation of benzylsilane **4** by reductive conversion of benzyl chloride and chlorosilane **2**. Using identical reaction conditions with chlorosilane **2** instead of hydrosilane **1**, the reductive coupling yielded 19% of benzylsilane **4** with subsequent chlorination of solvent. While the reductive route is a possible pathway to the benzylsilane, higher yields without solvent chlorination can only be achieved via the oxidative synthesis route, indicating the chlorosilane species not to be an essential intermediate.

We further investigated the influence of current density and electrode material, confirming the optimal conditions at 10 mA/cm² (see Supporting Information). Leaded bronze combines the advantages of high overpotential for hydrogen evolution, as

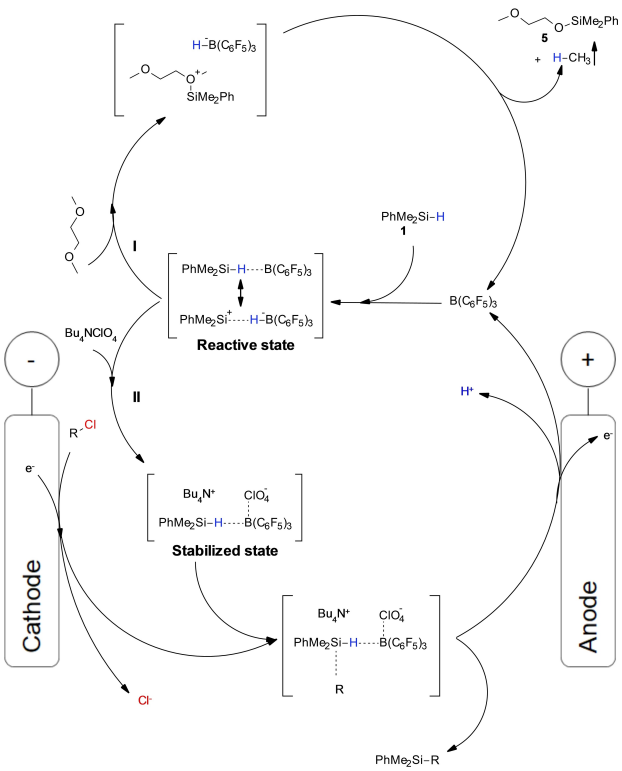

Scheme 4. Proposed mechanism for the anion stabilized and non-stabilized reaction pathway for the activated hydrosilane.

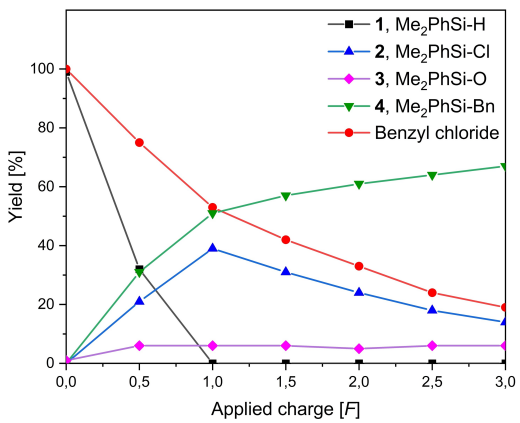

Figure 1. Distribution of components for the $B(C_6F_5)_3$-catalyzed benzylation of Me_2PhSiH in the course of electrolysis with **1**, $Me_2PhSi–H$ (black), **2**, $Me_2PhSi–Cl$ (blue), **3**, $Me_2PhSi–O–SiMe_2Ph$ (magenta), **4**, $Me_2PhSi–Bn$ (green) and benzyl chloride (red). Reaction conditions: current density of 10 mA/cm², 1,2-dimethoxyethane as solvent with 0.12 M Bu_4NClO_4 supporting electrolyte, anode material is glassy carbon, cathode material is CuSn7Pb15, Me_2PhSiH (0.50 M, 2.5 mmol) and benzyl chloride (0.69 M, 3.43 mmol), 1 mol% $B(C_6F_5)_3$ catalyst, at room temperature.

© 2022 The Authors. ChemElectroChem published by Wiley-VCH GmbH

21960216, 2022, 17, Downloaded from https://chemistry-europe.onlinelibrary.wiley.com/doi/10.1002/celc.202200840 by Universitatsbibliothek Mainz, Wiley Online Library on [27/01/2023]. See the Terms and Conditions (https://onlinelibrary.wiley.com/terms-and-conditions) on Wiley Online Library for rules of use; OA articles are governed by the applicable Creative Commons License

well as outstanding chemical and mechanical stability, that diminishes contamination of the product mixture by heavy metals at a low cost of 6–12 €/kg.[54] Furthermore, leaded bronzes have demonstrated to be more stable towards cathodic corrosion.[55] In addition to the hitherto used CuSn7Pb15 composition, we have investigated different variations of leaded bronzes, as well as their neat components as cathode materials (Table 2). Lead as cathode material suffers from corrosion, contaminating the supporting electrolyte with 600 ppm lead in course of reaction while shifting the product distribution to chlorosilane **2** as main product with 56% (Table 2, entry 1). Copper, as alloy matrix of leaded bronze, is corrosion resistant under these reaction conditions and yields benzylsilane **4** close to the amount for leaded bronzes with a shifted ratio favoring chlorosilane **2** (Table 2, entry 2). Interestingly, with rising amount of tin in the composition of leaded bronzes, the yield of Si–C bond formation increases with a maximum yield of 71% for CuSn10Pb10 (Table 2, entries 4–6). This can be even raised using a tin cathode, generating 86% of benzylsilane **4** and rendering the formation of chlorosilane **2** a minor side reaction (Table 2, entry 3). It should be noted, that while no visible corrosion of the tin electrode occurs, contamination of the supporting electrolyte with tin (16 ppm) is detectable after conversion. For the leaded bronze compositions, no contamination of the electrolyte by heavy metals was detectable.

Table 2. Product yield for the variation of cathode material for the activated oxidative Si–C bond formation with benzyl chloride.

Entry	Cathode material	Si–C, **4** Yield[b]	Si–Cl, **2** Yield[b]	Si–O, **3** Yield[b]	Conversion[a]
1[c]	Pb	28%	56%	9%	100%
2	Cu	60%	33%	4%	100%
3[d]	Sn	86%	8%	6%	100%
4	CuSn5Pb20	65%	27%	7%	100%
5	CuSn7Pb15	67%	21%	8%	100%
6	CuSn10Pb10	71%	23%	4%	100%

[a] Reaction conditions: current density of 10 mA/cm², applied charge of 3.0 *F*, 1,2-dimethoxyethane as solvent with 0.12 M Bu_4NClO_4 supporting electrolyte, anode material is glassy carbon, Me_2PhSiH (0.50 M, 2.5 mmol) and benzyl chloride (0.69 M, 3.43 mmol), 1 mol% $B(C_6F_5)_3$ catalyst, at room temperature. [b] Yield determined by NMR referenced to TMS; Si–C, 4 = benzyldimethylphenylsilane; Si–Cl, 2 = chlorodimethylphenylsilane; Si–O, 3 = tetramethyldiphenyldisiloxane. [c] 600 ppm Pb detectable in the electrolyte after conversion. [d] 16 ppm Sn detectable in the electrolyte after conversion.

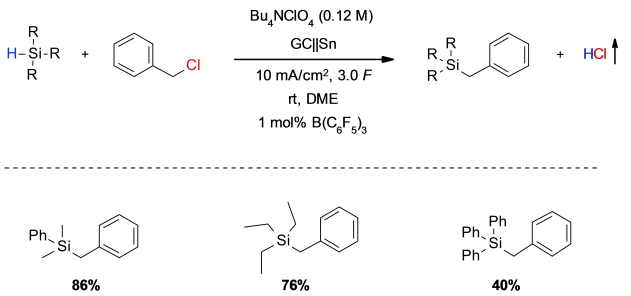

Scheme 5. Scope of electrochemical hydrosilane benzylation, yield determined by NMR referenced to TMS, GC = glassy carbon, DME = 1,2-dimethoxyethane.

The concept of boron-catalyzed electrochemical oxidative Si–C bond formation can be extended to alkylated and arylated hydrosilanes (Scheme 5). With increasing steric demand, the yield of Si–C bond formation diminishes, whereas the amount of chlorosilane rises.

Aside from the hitherto shown benzylation of hydrosilanes we further studied the allylation reaction. In this case, formation of the Si–C bond is made possible by the use of $B(C_6F_5)_3$, as underlined by cyclic voltammetry measurements (Figure 2). Hydrosilane **1** is oxidized in an irreversible process with a peak potential of 2.07 V vs. FcH/FcH^+. In comparison the product allyldimethylphenylsilane (Me_2PhSi-Allyl, **6**) is already oxidized at a peak potential of 1.49 V vs. FcH/FcH^+. In synthesis, the allylsilane can thus only be detected in traces. Preferential oxidation of the product compared to the starting material does not allow product accumulation. By oxidation of the allyl moiety, increasing amounts of disiloxane **3** and chlorosilane **2** are formed in course of reaction by electrolyte decomposition.

In presence of 1 mol% $B(C_6F_5)_3$, two additional oxidation potentials arise, shifting the onset potential by 880 mV, leading to oxidation potentials of 1.19 V vs. FcH/FcH^+ and 1.40 V vs. FcH/FcH^+. The oxidation potential of $[HB(C_6F_5)_3]^-$ is reported to be at 0.88 V vs. FcH/FcH^+,[29] differing from the obtained data by 310 mV. This indicates that complete hydride abstraction and availability of free $[HB(C_6F_5)_3]^-$ might not be the case in a perchlorate containing electrolyte. As discussed previously,[34] elongation of the Si–H bond without hydride abstraction should shift the oxidation potential of the formed adduct to less positive potentials due to decreasing activation barrier for Si–H cleavage. Here, it appears to correspond to an elongation of the Si–H bond without abstraction of hydride, since the reactivity of $B(C_6F_5)_3$ is decreased by the anion of the supporting electrolyte. Investigation of substrate stoichiometry indicated that an excess of 1.5 to 1.0 of hydrosilane **1** to allyl chloride allows for the highest yields for allylation reaction (see Supporting Information). For deeper insight into the reaction process and conversion, the reaction mixture was analyzed with

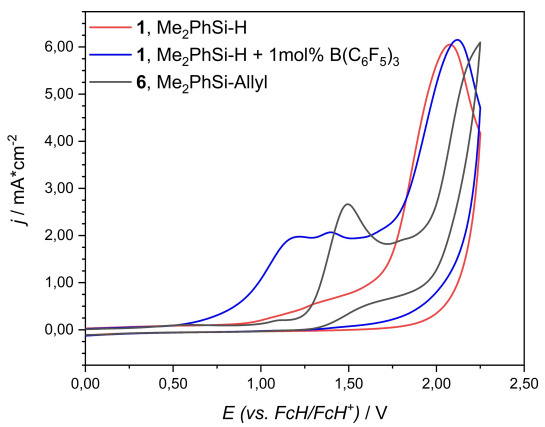

Figure 2. Cyclic voltammogram of 40 mM **1**, Me_2PhSiH (red), **1**, Me_2PhSiH with 1 mol% $B(C_6F_5)_3$ (blue) and **6**, Me_2PhSi-Allyl (black) in 0.1 M Bu_4NClO_4 and γ-butyrolactone. W.E. glassy carbon (A = 8.0 mm²), sweep rate $\nu = 0.2$ V/s.

© 2022 The Authors. ChemElectroChem published by Wiley-VCH GmbH

21960216, 2022, 17, Downloaded from https://chemistry-europe.onlinelibrary.wiley.com/doi/10.1002/celc.202200840 by Universitatsbibliothek Mainz, Wiley Online Library on [27/01/2023]. See the Terms and Conditions (https://onlinelibrary.wiley.com/terms-and-conditions) on Wiley Online Library for rules of use; OA articles are governed by the applicable Creative Commons License

increasing applied charge by GC and NMR. The emerging distribution can be divided into three parts (Figure 3).

In the first part of the reaction progress, until 1.0 *F* of applied charge is transferred, hydrosilane **1** is oxidatively consumed to form chlorosilane **2** as main product as well as allylsilane **6** as byproduct. Disiloxane **3** is generated by initial decomposition with the supporting electrolyte and yield does barely increase until 1.0 *F* applied charge is exceeded. At 1.0 *F* the maximum yield of allylsilane **6** is reached with 35% and hydrosilane **1** is completely consumed.

For the second part, due to the absence of a hydrosilane, allylsilane **6** is now the oxidatively consumed species, diminishing its yield and generating chlorosilane **2** as well as disiloxane **3**. Between 2.0 and 2.5 *F* allylsilane **6** is completely consumed and the yield of chlorosilane **2** reaches its maximum with 65%. The third part is initialized and due to missing alternative species, anodic halogenation of supporting electrolyte occurs

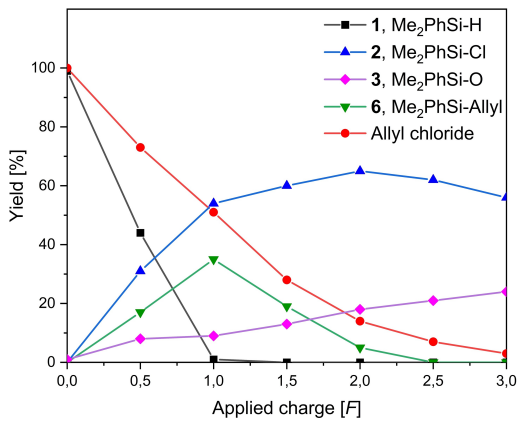

Figure 3. Distribution of components for the $B(C_6F_5)_3$-catalyzed allylation of Me_2PhSiH in the course of electrolysis with **1**, Me_2PhSi–H (black), **2**, Me_2PhSi–Cl (blue), **3**, Me_2PhSi–O–$SiMe_2Ph$ (magenta), **6**, Me_2PhSi-Allyl (green) and allyl chloride (red). Reaction conditions: current density of 10 mA/cm^2, 1,2-dimethoxyethane as solvent with 0.12 M Bu_4NClO_4 supporting electrolyte, anode material is glassy carbon, cathode material is CuSn7Pb15, Me_2PhSiH (0.50 M, 2.50 mmol) and allyl chloride (0.33 M, 1.67 mmol), 1 mol% $B(C_6F_5)_3$ catalyst, at room temperature.

Table 3. Product yield for the variation of cathode material for the activated oxidative Si–C bond formation with allyl chloride.

Entry	Cathode material	Si–C, **6** Yield[b]	Si–Cl, **2** Yield[b]	Si–O, **3** Yield[b]	Conversion[a]
1[c]	Pb	34%	54%	9%	100%
2	Cu	31%	57%	7%	100%
3[d]	Sn	8%	77%	8%	100%
4	CuSn5Pb20	30%	60%	9%	100%
5	CuSn7Pb15	35%	54%	9%	100%
6	CuSn10Pb10	29%	57%	9%	100%

[a] Reaction conditions: current density of 10 mA/cm^2, applied charge of 1.0 *F*, 1,2-dimethoxyethane as solvent with 0.12 M Bu_4NClO_4 supporting electrolyte, anode material is glassy carbon, Me_2PhSiH (0.50 M, 2.50 mmol) and allyl chloride (0.33 M, 1.67 mmol), 1 mol% $B(C_6F_5)_3$ catalyst, at room temperature. [b] Yield determined by NMR referenced to TMS; Si–C, 6 = allyldimethylphenylsilane; Si–Cl, 2 = chlorodimethylphenylsilane; Si–O, 3 = tetramethyldiphenyldisiloxane. [c] 400 ppm Pb detectable in the electrolyte after conversion. [d] 14 ppm Sn detectable in the electrolyte after conversion.

while chlorosilane **2** is reduced by cathodic reduction with consecutive formation of disiloxane **3** as thermodynamic sink. It should be noted that no further generation of allylsilane by reductive coupling of allyl chloride with chlorosilane **2** is detectable.

These observations support the suggestion that for borane-activated electrochemical Si–C bond formation, a one-electron process could occur for the conversion of intermediate. Furthermore, since the product is prone to oxidation, the maximum yield cannot be increased after complete conversion of the starting hydrosilane.

Analogue to materials chosen for the benzylation reaction, a screening of electrode material was conducted. For the allylation reaction lead and the leaded bronze CuSn7Pb15 generate the highest yield of allylsilane **6** with 35% (Table 3, entries 1 and 5). For lead, visible corrosion of the electrode material occurs and contamination of the supporting electrolyte by lead (400 ppm) is detectable after conversion. Tin as the most promising material for the benzylation of hydrosilanes is not suitable for the allylation reaction, diminishing the yield for allylsilane **6** to 8% and favoring the Si–Cl bond formation towards chlorosilane **2** (Table 3, entry 3). Furthermore, contamination of the supporting electrolyte by 14 ppm tin is determined. The leaded bronze alloys CuSn5Pb20 and CuSn10Pb10 show comparable results to the copper cathode, with formation of allylsilane **6** in the range of 29–31%, as well as yields determined for chlorosilane **2** and disiloxane **3** (Table 3, entries 2, 4 and 6). Increase of lead content to a maximum amount of 20% for CuSn5Pb20 does not increase the yield compared to CuSn7Pb15, rendering CuSn7Pb15 as preferred cathode material for the allylation of hydrosilanes without contamination of the supporting electrolyte by heavy metals.

Like the benzylation of hydrosilanes, this concept can be extended to alkylated and arylated hydrosilanes (Scheme 6). Again, increasing steric demand diminishes the yield of Si–C bond formation and raises the amount of chlorosilane.

Product distribution for the allylation reaction shows, that chlorination of the reactive silyl intermediate is one major side reaction, leading to the respective chlorosilanes. Hydrogen chloride released in course of reaction might be mainly responsible for the generation of chlorosilane species, diminishing the preferred Si–C bond formation. We therefore tried

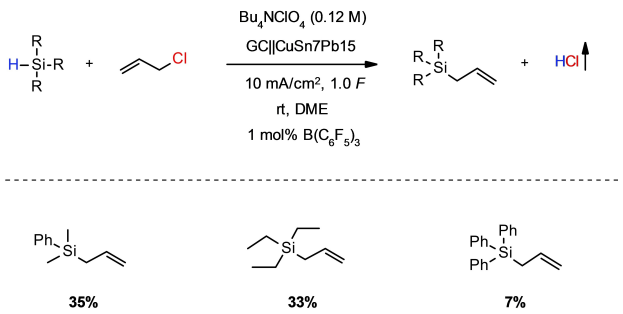

Scheme 6. Product scope of hydrosilane allylation, yield determined by NMR referenced to TMS, GC = glassy carbon, DME = 1,2-dimethoxyethane.

© 2022 The Authors. ChemElectroChem published by Wiley-VCH GmbH

21960216, 2022, 17, Downloaded from https://chemistry-europe.onlinelibrary.wiley.com/doi/10.1002/celc.202200840 by Universitatsbibliothek Mainz, Wiley Online Library on [27/01/2023]. See the Terms and Conditions (https://onlinelibrary.wiley.com/terms-and-conditions) on Wiley Online Library for rules of use; OA articles are governed by the applicable Creative Commons License

21960216, 2022, 17, Downloaded from https://chemistry-europe.onlinelibrary.wiley.com/doi/10.1002/celc.202200840 by Universitatsbibliothek Mainz, Wiley Online Library on [27/01/2023]. See the Terms and Conditions (https://onlinelibrary.wiley.com/terms-and-conditions) on Wiley Online Library for rules of use; OA articles are governed by the applicable Creative Commons License

various approaches to eliminate the released hydrogen chloride from the reaction mixture and to increase the amount of Si–C bond formation. Different scavenging strategies like precipitation of insoluble chloride salts, ion exchange as well as addition reactions involving epoxides were used (see Supporting Information). While the amount of chlorosilane **2** could be diminished, the yield of allylsilane **6** and the conversion of hydrosilane **1** was reduced as well, indicating anodic competition reactions and inactivation of $B(C_6F_5)_3$.

The electrochemical reaction of hydrosilanes with organic halides under borane-catalyzed conditions can be well demonstrated by the systems of benzyl and allyl species. These exhibit high stabilization of the anionic intermediate and show relatively low reduction potentials. However, extension of the scope quickly shows limits if reduction potential or stabilization of the intermediate are not sufficient. Using halo benzenes, the respective Si–C bond formation and complete conversion of hydrosilane can be achieved, yet the yield of the desired phenylsilane is rather low and cannot be increased by the use of $B(C_6F_5)_3$. Changing the halide species from chlorobenzene to bromo and iodobenzene does not change the yield in relation to the decreasing reduction potential. If the stabilization of the anion is increased by electron-withdrawing substituents, such as cyano groups, there is also no increase in yield. 4-Chloro- and 4-bromobenzonitrile show relatively low reduction potentials, cathodic access is thus possible and the conversion of the hydrosilane is 100% (see Supporting Information). However, stabilization of negative charge by resonance remains crucial for successful conversion so far.

Conclusion

The first boron-catalyzed electrochemical Si–C bond formation was established. By application of only catalytic amounts in the range of 1 mol% of Lewis acidic boranes such as $B(C_6F_5)_3$, benzylation and allylation of hydrosilanes were achieved in yields up to 86%. Cyclic voltammetry studies demonstrated that $B(C_6F_5)_3$ could be assigned the role to activate the hydrosilane for easier oxidation in presence of supporting electrolyte, resulting in significant increase in yield and the enrichment of the target product. Subsequent oxidation of product could be successfully suppressed by the shift of oxidation potential achieved by activation of hydrosilane with the Lewis acidic borane. The conversion was not only safe and easily controllable, but also cost-effective due to the use of glassy carbon and leaded bronze as electrode materials. Leaded bronze as cathode materials showed superior properties for this application and prevented contamination of the electrolyte with heavy metals. The scope of substrates has thus far been successfully applied only to benzyl and allyl chloride. However, we are convinced that further suitable substrates will be found in the near future to enrich the opportunity of electrochemical borane-catalyzed Si–C bond formation.

Experimental Section

Synthesis of material

For screening experiments undivided (5 mL) PTFE cells for electrolysis with reaction block, stirrer, power supply were obtained as IKA Screening System (IKA-Werke GmbH & Co. KG, Staufen, Germany). The active surface of the respective used electrode was 1.3 cm^2, anode and cathode surface were separated by 0.5 cm. The software used was IKA Labworldsoft 6.0.

Electrochemical benzylation of hydrosilanes

The undivided cell compartment was charged with $B(C_6F_5)_3$ (12.8 mg, $2.5\cdot10^{-2}$ mmol, $1.0\cdot10^{-2}$ eq.), DME (5.0 mL) and Bu_4NClO_4 (205 mg, 0.12 M). Me_2PhSiH (383.2 μL, 2.5 mmol, 1.0 eq.) and benzyl chloride (394.7 μL, 3.4 mmol, 1.3 eq.) were added under stirring (500 rpm). The electrodes were connected to the IKA power supply, and the reaction was conducted at room temperature ($j = 10$ mA/cm^2, 3.0 *F*). The general workup procedure consisted of stripping off volatile compounds. Chlorosilanes were distilled under inert gas atmosphere. Organosilanes were further purified by washing of the organic layer with distilled water (3×25 mL) and back-washing with n-pentane (3×25 mL). The combined organic fractions were dried over Na_2SO_4 and filtered. Volatile compounds were stripped off and the crude product was purified by column chromatography.

Electrochemical allylation of hydrosilanes

The undivided cell compartment was charged with $B(C_6F_5)_3$ (12.8 mg, $2.5\cdot10^{-2}$ mmol, $1.0\cdot10^{-2}$ eq.), DME (5.0 mL) and Bu_4NClO_4 (205 mg, 0.12 M). Me_2PhSiH (383.2 μL, 2.5 mmol, 1.0 eq.) and allyl chloride (135.7 μL, 1.7 mmol, 0.7 eq.) were added under stirring (500 rpm). The electrodes were connected to the IKA power supply, and the reaction was conducted at room temperature ($j = 10$ mA/cm^2, 1.0 *F*). The workup procedure was analogue to the synthesis of benzylsilanes.

Characterization

NMR Spectroscopy of ^1H, ^{13}C and ^{29}Si spectra were recorded at 25 °C, using a Bruker Avance 500 (500 MHz, Analytische Messtechnik, Karlsruhe, Germany). Chemical shifts (δ) are reported in parts per million (ppm). Traces of CH_2Cl_2 in the corresponding deuterated solvent, or tetramethylsilane for ^{29}Si spectra were used as internal standard for calibration. GC-MS measurements were carried out on an Agilent GC-A6890 N using a HP-5 column (Agilent Technologies, Santa Clara, California), length: 30 m, inner diameter: 0.25 mm, film: 0.25 μm, carrier gas: helium. The chromatograph was coupled to a mass spectrometer Agilent MSD 5975 C (Agilent, Santa Clara, California, USA).

Allyldimethylphenylsilane: ^1H NMR (500 MHz, CD_2Cl_2): δ [ppm] = 7.68–7.72 (m, 5H), 5.87–5.99 (m, 1H), 4.95–5.04 (m, 2H), 1.91 (d, J = 8.0 Hz, 2H), 0.43 (s, 6H). ^{13}C NMR (125 MHz, CD_2Cl_2): δ [ppm] = 140.1, 135.0, 133.9, 129. 6, 128.0, 113.5, 23.9, −3.4. ^{29}Si NMR (100 MHz, CD_2Cl_2): δ [ppm] = −4.72. MS m/z = 176 $[M]^+$.

Allyltriethylsilane: ^1H NMR (500 MHz, CD_2Cl_2): δ [ppm] = 6.03–6.22 (m, 1H), 5.56–5.74 (m, 2H), 1.86 (d, J = 8.0 Hz, 2H), 0.99 (t, J = 7.8 Hz, 9H), 0.43–0.65 (m, 6H). ^{13}C NMR (125 MHz, CD_2Cl_2): δ [ppm] = 127.6, 112.5, 18.5, 7.4, 3.1. ^{29}Si NMR (100 MHz, CD_2Cl_2): δ [ppm] = 5.74. MS m/z = 156 $[M]^+$.

Allyltriphenylsilane: ^1H NMR (500 MHz, CD_2Cl_2): δ [ppm] = 7.52–7.58 (m, 6H), 7.36–7.48 (m, 9H), 5.85–5.95 (m, 1H), 4.88–5.00 (m, 2H), 2.45

© 2022 The Authors. ChemElectroChem published by Wiley-VCH GmbH

(d, $J=8.0$ Hz, 2H). ^{13}C NMR (125 MHz, CD_2Cl_2): δ [ppm] = 135.7, 134.6, 133.9, 129.6, 127.8, 114.8, 21.0. ^{29}Si NMR (100 MHz, CD_2Cl_2): δ [ppm] = −13.73. MS m/z = 301 $[M]^+$.

Benzyldimethylphenylsilane: ^1H NMR (500 MHz, CD_2Cl_2): δ [ppm] = 7.58–7.68 (m, 2H), 7.40–7.50 (m, 3H), 7.31 (t, $J=7.6$ Hz, 2H), 7.20 (t, $J=7.4$ Hz, 1H), 7.10 (d, $J=7.6$ Hz, 2H), 2.47 (s, 2H), 0.41 (s, 6H). ^{13}C NMR (125 MHz, CD_2Cl_2): δ [ppm] = 139.9, 138.6, 133.9, 129.1, 128.4, 128.2, 127.8, 124.2, 26.1, −3.5. ^{29}Si NMR (100 MHz, CD_2Cl_2): δ [ppm] = −3.76. MS m/z = 226 $[M]^+$.

Benzyltriethylsilane: ^1H NMR (500 MHz, CD_2Cl_2): δ [ppm] = 7.22–7.27 (m, 2H), 7.06–7.11 (m, 3H), 2.18 (s, 2H), 0.99 (t, $J=8.0$ Hz, 9H), 0.51 (q, $J=8.0$ Hz, 6H). ^{13}C NMR (125 MHz, CD_2Cl_2): δ [ppm] = 141.2, 129.0, 128.5, 124.2, 21.9, 7.5, 3.4. ^{29}Si NMR (100 MHz, CD_2Cl_2): δ [ppm] = 6.41. MS m/z = 206 $[M]^+$.

Benzyltriphenylsilane: ^1H NMR (500 MHz, CD_2Cl_2): δ [ppm] = 7.53–7.59 (m, 6H), 7.42–7.47 (m, 9H), 7.12–7.22 (m, 2H), 6.99–7.03 (m, 3H), 3.10 (s, 2H). ^{13}C NMR (125 MHz, CD_2Cl_2): δ [ppm] = 138.5, 136.0, 134.4, 129.3, 129.1, 128.2, 127.9, 124.7, 23.3. ^{29}Si NMR (100 MHz, CD_2Cl_2): δ [ppm] = −12.26. MS m/z = 350 $[M]^+$.

Chlorodimethylphenylsilane: ^1H NMR (500 MHz, CD_2Cl_2): δ [ppm] = 7.71–7.74 (m, 2H), 7.46–7.54 (m, 3H), 0.77 (s, 6H). ^{13}C NMR (125 MHz, CD_2Cl_2): δ [ppm] = 136.7, 133.5, 130.8, 128.5, 2.2. ^{29}Si NMR (100 MHz, CD_2Cl_2): δ [ppm] = 20.49. MS m/z = 170 $[M]^+$.

Dimethyloctylphenylsilane: ^1H NMR (500 MHz, CD_2Cl_2): δ [ppm] = 7.46–7.55 (m, 2H), 7.29–7.37 (m, 3H), 1.18–1.40 (m, 12H), 0.85 (t, $J=6.9$ Hz, 3H), 0.72–0.78 (m, 2H), 0.22 (s, 6H). ^{13}C NMR (125 MHz, CD_2Cl_2): δ [ppm] = 139.8, 133.7, 128.8, 127.8, 33.8, 32.1, 29.4, 24.0, 22.8, 15.9, 14.3, −2.8. ^{29}Si NMR (100 MHz, CD_2Cl_2): δ [ppm] = −2.41. MS m/z = 248 $[M]^+$.

Dimethyldiphenylsilane: ^1H NMR (500 MHz, CD_2Cl_2): δ [ppm] = 7.50–7.59 (m, 4H), 7.29–7.44 (m, 6H), 0.48 (s, 6H). ^{13}C NMR (125 MHz, CD_2Cl_2): δ [ppm] = 137.9, 134.0, 128.7, 127.3, −3.0. ^{29}Si NMR (100 MHz, CD_2Cl_2): δ [ppm] = −8.17. MS m/z = 212 $[M]^+$.

4-(Dimethylphenylsilyl)benzonitrile: ^1H NMR (500 MHz, CD_2Cl_2): δ [ppm] = 7.62–7.69 (m, 4H), 7.51–7.56 (m, 2H), 7.31–7.40 (m, 3H), 0.43 (s, 6H). ^{13}C NMR (125 MHz, CD_2Cl_2): δ [ppm] = 145.2, 136.6, 134.8, 134.3, 131.2, 129.8, 128.3, 119.1, 112.9, −2.5. ^{29}Si NMR (100 MHz, CD_2Cl_2): δ [ppm] = −7.12. MS m/z = 237 $[M]^+$.

1,1,3,3-tetramethyl-1,3-diphenyldisiloxane: ^1H NMR (500 MHz, CD_2Cl_2): δ [ppm] = 7.58–7.63 (m, 4H), 7.36–7.44 (m, 6H), 0.40 (s, 12H). ^{13}C NMR (125 MHz, CD_2Cl_2): δ [ppm] = 140.2, 133.4, 129.6, 128.0, 0.9. ^{29}Si NMR (100 MHz, CD_2Cl_2): δ [ppm] = −1.08. MS m/z = 286 $[M]^+$.

(2-Methoxyethoxy)dimethylphenylsilane: ^1H NMR (500 MHz, CD_2Cl_2): δ [ppm] = 7.60–7.67 (m, 2H), 7.38–7.47 (m, 3H), 3.80 (t, $J=5.0$ Hz, 2H), 3.52 (t, $J=5.0$ Hz, 2H), 3.39 (s, 3H), 0.45 (s, 6H). ^{13}C NMR (125 MHz, CD_2Cl_2): δ [ppm] = 138.3, 133.8, 129.9, 128.1, 74.6, 62.6, 59.3, −1.7. ^{29}Si NMR (100 MHz, CD_2Cl_2): δ [ppm] = 7.72. MS m/z = 195 $[M–CH_3]^+$.

Further detailed information on general procedures, electrochemical conversions, cyclic voltammetry measurements and product characterization can be found in the Supporting Information.

Acknowledgements

Open Access funding enabled and organized by Projekt DEAL.

Conflict of Interest

The authors declare no conflict of interest.

Data Availability Statement

The data that support the findings of this study are available in the supplementary material of this article.

Keywords: Boron · Electrolysis · Lewis acid activation · Oxidative coupling · Silicon

[1] V. Gevorgyan, M. Rubin, S. Benson, J.-X. Liu, Y. Yamamoto, *J. Org. Chem.* **2000**, *65*, 6179–6186.
[2] a) V. Gevorgyan, J.-X. Liu, Y. Yamamoto, *Chem. Commun.* **1998**, 37–38; b) R. L. Melen, *Chem. Commun.* **2014**, *50*, 1161–1174; c) D. J. Morrison, J. M. Blackwell, W. E. Piers, *Pure Appl. Chem.* **2004**, *76*, 615–623; d) D. J. Morrison, W. E. Piers, *Org. Lett.* **2003**, *5*, 2857–2860.
[3] a) A. Bernsdorf, H. Brand, R. Hellmann, M. Köckerling, A. Schulz, A. Villinger, K. Voss, *J. Am. Chem. Soc.* **2009**, *131*, 8958–8970; b) I. Krossing, I. Raabe, *Angew. Chem. Int. Ed.* **2004**, *43*, 2066–2090; *Angew. Chem.* **2004**, *116*, 2116–2142; c) S. J. Lancaster, A. Rodriguez, A. Lara-Sanchez, M. D. Hannant, D. A. Walker, D. H. Hughes, M. Bochmann, *Organometallics* **2002**, *21*, 451–453; d) R. E. LaPointe, G. R. Roof, K. A. Abboud, J. Klosin, *J. Am. Chem. Soc.* **2000**, *122*, 9560–9561; e) X. Yang, C. L. Stern, T. J. Marks, *J. Am. Chem. Soc.* **1994**, *116*, 10015–10031.
[4] a) A. G. Massey, A. J. Park, *J. Organomet. Chem.* **1964**, *2*, 245–250; b) A. G. Massey, A. J. Park, *J. Organomet. Chem.* **1966**, *5*, 218–225; c) A. G. Massey, A. J. Park, F. G. A. Stone, *Proc. Chem. Soc.* **1963**, *212*.
[5] a) M. A. Beckett, D. S. Brassington, S. J. Coles, M. B. Hursthouse, *Inorg. Chem. Commun.* **2000**, *3*, 530–533; b) H. Jacobsen, H. Berke, S. Döring, G. Kehr, G. Erker, R. Fröhlich, O. Meyer, *Organometallics* **1999**, *18*, 1724–1735.
[6] D. W. Stephan, G. Erker, *Angew. Chem. Int. Ed.* **2015**, *54*, 6400–6441; *Angew. Chem.* **2015**, *127*, 6498–6541.
[7] D. W. Stephan, *Science* **2016**, *354*, aaf7229.
[8] a) L. Greb, P. Oña-Burgos, B. Schirmer, S. Grimme, D. W. Stephan, J. Paradies, *Angew. Chem. Int. Ed.* **2012**, *51*, 10164–10168; *Angew. Chem.* **2012**, *124*, 10311–10315; b) D. W. Stephan, G. Erker, *Angew. Chem. Int. Ed.* **2010**, *49*, 46–76; *Angew. Chem.* **2010**, *122*, 50–81; c) G. C. Welch, D. W. Stephan, *J. Am. Chem. Soc.* **2007**, *129*, 1880–1881.
[9] D. W. Stephan, G. Erker, *Chem. Sci.* **2014**, *5*, 2625–2641.
[10] R. Dobrovetsky, D. W. Stephan, *J. Am. Chem. Soc.* **2013**, *135*, 4974–4977.
[11] C. M. Mömming, E. Otten, G. Kehr, R. Fröhlich, S. Grimme, D. W. Stephan, G. Erker, *Angew. Chem. Int. Ed.* **2009**, *48*, 6643–6646; *Angew. Chem.* **2009**, *121*, 6770–6773.
[12] A. Y. Houghton, J. Hurmalainen, A. Mansikkamäki, W. E. Piers, H. M. Tuononen, *Nat. Chem.* **2014**, *6*, 983–988.
[13] D. J. Parks, J. M. Blackwell, W. E. Piers, *J. Org. Chem.* **2000**, *65*, 3090–3098.
[14] J. M. Blackwell, E. R. Sonmor, T. Scoccitti, W. E. Piers, *Org. Lett.* **2000**, *2*, 3921–3923.
[15] W. E. Piers, A. J. V. Marwitz, L. G. Mercier, *Inorg. Chem.* **2011**, *50*, 12252–12262.
[16] T. Hackel, N. A. McGrath, *Molecules* **2019**, *24*, 432.
[17] D. T. Hog, M. Oestreich, *Eur. J. Org. Chem.* **2009**, *2009*, 5047–5056.
[18] J. M. Blackwell, K. L. Foster, V. H. Beck, W. E. Piers, *J. Org. Chem.* **1999**, *64*, 4887–4892.
[19] D. J. Parks, W. E. Piers, *J. Am. Chem. Soc.* **1996**, *118*, 9440–9441.
[20] M. Rubin, T. Schwier, V. Gevorgyan, *J. Org. Chem.* **2002**, *67*, 1936–1940.
[21] W. Yuan, P. Smirnov, M. Oestreich, *Chem* **2018**, *4*, 1443–1450.
[22] J. M. Blackwell, D. J. Morrison, W. E. Piers, *Tetrahedron* **2002**, *58*, 8247–8254.
[23] a) J. Hermeke, M. Mewald, M. Oestreich, *J. Am. Chem. Soc.* **2013**, *135*, 17537–17546; b) K. Müther, J. Mohr, M. Oestreich, *Organometallics* **2013**, *32*, 6643–6646.
[24] S. Rendler, M. Oestreich, *Angew. Chem. Int. Ed.* **2008**, *47*, 5997–6000; *Angew. Chem.* **2008**, *120*, 6086–6089.

© 2022 The Authors. ChemElectroChem published by Wiley-VCH GmbH

21960216, 2022, 17, Downloaded from https://chemistry-europe.onlinelibrary.wiley.com/doi/10.1002/celc.202200840 by Universitatsbibliothek Mainz, Wiley Online Library on [27/01/2023]. See the Terms and Conditions (https://onlinelibrary.wiley.com/terms-and-conditions) on Wiley Online Library for rules of use; OA articles are governed by the applicable Creative Commons License

[25] K. Chulsky, R. Dobrovetsky, *Angew. Chem. Int. Ed.* **2017**, *56*, 4744–4748; *Angew. Chem.* **2017**, *129*, 4822–4826.
[26] W. Yang, L. Gao, J. Lu, Z. Song, *Chem. Commun.* **2018**, *54*, 4834–4837.
[27] S. A. Cummings, M. Iimura, C. J. Harlan, R. J. Kwaan, I. V. Trieu, J. R. Norton, B. M. Bridgewater, F. Jäkle, A. Sundararaman, M. Tilset, *Organometallics* **2006**, *25*, 1565–1568.
[28] E. J. Lawrence, V. S. Oganesyan, G. G. Wildgoose, A. E. Ashley, *Dalton Trans.* **2013**, *42*, 782–789.
[29] E. J. Lawrence, V. S. Oganesyan, D. L. Hughes, A. E. Ashley, G. G. Wildgoose, *J. Am. Chem. Soc.* **2014**, *136*, 6031–6036.
[30] E. J. Lawrence, T. J. Herrington, A. E. Ashley, G. G. Wildgoose, *Angew. Chem. Int. Ed.* **2014**, *53*, 9922–9925; *Angew. Chem.* **2014**, *126*, 10080–10083.
[31] Y. M. Lee, J. E. Seo, N.-S. Choi, J.-K. Park, *Electrochim. Acta* **2005**, *50*, 2843–2848.
[32] G.-B. Han, J.-N. Lee, J. W. Choi, J.-K. Park, *Electrochim. Acta* **2011**, *56*, 8997–9003.
[33] a) C.-C. Chang, T.-K. Chen, *J. Power Sources* **2009**, *193*, 834–840; b) C.-C. Chang, T.-K. Chen, L.-J. Her, G. T.-K. Fey, *J. Electrochem. Soc.* **2009**, *156*, A828-A832.
[34] A. D. Beck, S. Haufe, J. Tillmann, S. R. Waldvogel, *ChemElectroChem* **2022**, *9*, e202101374.
[35] a) A. Hosomi, *Acc. Chem. Res.* **1988**, *21*, 200–206; b) H. Sakurai, *Pure Appl. Chem.* **1982**, *54*, 1–22.
[36] A. Ramirez, K. A. Woerpel, *Org. Lett.* **2005**, *7*, 4617–4620.
[37] Z. Li, X. Cao, G. Lai, J. Liu, Y. Ni, J. Wu, H. Qiu, *J. Organomet. Chem.* **2006**, *691*, 4740–4746.
[38] R. E. Grote, E. R. Jarvo, *Org. Lett.* **2009**, *11*, 485–488.
[39] T. Shono, Y. Matsumura, S. Katoh, N. Kise, *Chem. Lett.* **1985**, *14*, 463–466.
[40] J. Yoshida, K. Muraki, H. Funahashi, N. Kawabata, *J. Org. Chem.* **1986**, *51*, 3996–4000.
[41] J. Yoshida, K. Muraki, H. Funahashi, N. Kawabata, *J. Organomet. Chem.* **1985**, *284*, C33-C35.
[42] a) G. Martin, F. S. Kipping, *J. Chem. Soc. Trans.* **1909**, *95*, 302–314; b) R. Robison, F. S. Kipping, *J. Chem. Soc. Trans.* **1908**, *93*, 439–456.
[43] Z.-D. Huang, R. Ding, P. Wang, Y.-H. Xu, T.-P. Loh, *Chem. Commun.* **2016**, *52*, 5609–5612.
[44] M. A. Brook, *Silicon in organic, organometallic, and polymer chemistry*, Wiley, New York, Weinheim, **2000**.
[45] a) D. Cantillo, *Chem. Commun.* **2022**, *58*, 619–628; b) C. Kingston, M. D. Palkowitz, Y. Takahira, J. C. Vantourout, B. K. Peters, Y. Kawamata, P. S. Baran, *Acc. Chem. Res.* **2020**, *53*, 72–83; c) M. C. Leech, K. Lam, *Nat. Chem. Rev.* **2022**, *6*, 275–286; d) R. D. Little, K. D. Moeller, *Chem. Rev.* **2018**, *118*, 4483–4484; e) S. Möhle, M. Zirbes, E. Rodrigo, T. Gieshoff, A. Wiebe, S. R. Waldvogel, *Angew. Chem. Int. Ed.* **2018**, *57*, 6018–6041; *Angew. Chem.* **2018**, *130*, 6124–6149; f) A. Shatskiy, H. Lundberg, M. D. Kärkäs, *ChemElectroChem* **2019**, *6*, 4067–4092; g) A. Wiebe, T. Gieshoff, S. Möhle, E. Rodrigo, M. Zirbes, S. R. Waldvogel, *Angew. Chem. Int. Ed.* **2018**, *57*, 5594–5619; *Angew. Chem.* **2018**, *130*, 5694–5721; h) M. Yan, Y. Kawamata, P. S. Baran, *Chem. Rev.* **2017**, *117*, 13230–13319.
[46] a) B. A. Frontana-Uribe, R. D. Little, J. G. Ibanez, A. Palma and R. Vasquez-Medrano, *Green Chem.* **2010**, *12*, 2099; b) D. Pollok, S. R. Waldvogel, *Chem. Sci.* **2020**, *11*, 12386–12400; c) J. Seidler, J. Strugatchi, T. Gärtner, S. R. Waldvogel, *MRS Energy Sustainability* **2020**, *7*, E42.
[47] a) J. L. Röckl, D. Pollok, R. Franke, S. R. Waldvogel, *Acc. Chem. Res.* **2020**, *53*, 45–61; b) S. R. Waldvogel, S. Lips, M. Selt, B. Riehl, C. J. Kampf, *Chem. Rev.* **2018**, *118*, 6706–6765.
[48] C. Grogger, B. Loidl, H. Stueger, T. Kammel, B. Pachaly, *J. Organomet. Chem.* **2006**, *691*, 105–110.
[49] a) A. Kunai, T. Kawakami, E. Toyoda, M. Ishikawa, *Organometallics* **1991**, *10*, 2001–2003; b) J. Ohshita, K. Hino, T. Iwawaki, A. Kunai, *J. Organomet. Chem.* **2009**, *625*, 138–143.
[50] a) E. Hengge, H. Firgoi, *J. Organomet. Chem.* **1981**, *212*, 155–161; b) E. Hengge, G. Litscher, *Angew. Chem. Int. Ed.* **1976**, *15*, 370; *Angew. Chem.* **1976**, *88*, 414.
[51] C. Jammegg, S. Graschy, E. Hengge, *Organometallics* **1994**, *13*, 2397–2400.
[52] A. Kunai, T. Kawakami, E. Toyoda, T. Sakurai, M. Ishikawa, *Chem. Lett.* **1993**, *22*, 1945–1948.
[53] M. Palframan, A. Parsons, P. Johnson, *Synlett* **2011**, *2011*, 2811–2814.
[54] a) C. Gütz, V. Grimaudo, M. Holtkamp, M. Hartmer, J. Werra, L. Frensemeier, A. Kehl, U. Karst, P. Broekmann, S. R. Waldvogel, *ChemElectroChem* **2018**, *5*, 247–252; b) C. Gütz, M. Selt, M. Bänziger, C. Bucher, C. Römelt, N. Hecken, F. Gallou, T. R. Galvão, S. R. Waldvogel, *Chem. Eur. J.* **2015**, *21*, 13878–13882.
[55] a) C. Gütz, M. Bänziger, C. Bucher, T. R. Galvão, S. R. Waldvogel, *Org. Process Res. Dev.* **2015**, *19*, 1428–1433; b) T. Wirtanen, T. Prenzel, J.-P. Tessonnier, S. R. Waldvogel, *Chem. Rev.* **2021**, *121*, 10241–10270; c) T. Wirtanen, E. Rodrigo, S. R. Waldvogel, *Chem. Eur. J.* **2020**, *26*, 5592–5597.

Manuscript received: August 9, 2022
Revised manuscript received: August 12, 2022
Accepted manuscript online: August 12, 2022

© 2022 The Authors. ChemElectroChem published by Wiley-VCH GmbH

21960216, 2022, 17, Downloaded from https://chemistry-europe.onlinelibrary.wiley.com/doi/10.1002/celc.202200840 by Universitatsbibliothek Mainz, Wiley Online Library on [27/01/2023]. See the Terms and Conditions (https://onlinelibrary.wiley.com/terms-and-conditions) on Wiley Online Library for rules of use; OA articles are governed by the applicable Creative Commons License